

Mechanism of the $^{93}\text{Nb}(\bar{p}, ^3\text{He})$ inclusive reaction at an incident energy of 160 MeV

A. A. Cowley* and J. J. van Zyl

Department of Physics, Stellenbosch University, Private Bag XI, Matieland, 7602, South Africa

S. S. Dimitrova

Institute for Nuclear Research and Nuclear Energy, Bulgarian Academy of Sciences, 1784 Sofia, Bulgaria

E. V. Zemlyanaya and K. V. Lukyanov

Joint Institute for Nuclear Research, 141980 Dubna, Russia

(Received 27 February 2012; published 30 May 2012)

The inclusive $^{93}\text{Nb}(\bar{p}, ^3\text{He})$ reaction to the continuum was investigated at an incident energy of 160 MeV. Emission-energy distributions for cross sections as well as analyzing powers were explored. A range of scattering angles from 15° to 60° (lab.) was covered and ^3He emission energies from ≈ 30 MeV to the kinematic limit were measured. As in our earlier work, the experimental distributions were compared with a multistep direct theory in which a reaction mechanism based on two-nucleon pickup is employed. Reasonable agreement between experimental double-differential cross sections and analyzing powers and the theoretical expectation was obtained. This work, together with published results for the same reaction at a lower projectile energy, allows the incident-energy dependence of the cross section and analyzing power distributions to be explored.

DOI: [10.1103/PhysRevC.85.054622](https://doi.org/10.1103/PhysRevC.85.054622)

PACS number(s): 25.40.Hs, 24.50.+g, 24.60.Gv, 24.70.+s

I. INTRODUCTION

Although nucleon-induced reactions into the continuum of emission energies have been studied for many years in the incident energy range of 100 to 200 MeV, there is still a surprising and disconcerting lack of insight regarding the reaction mechanism leading to composite ejectiles (see for example Ref. [1]). This situation is very frustrating, especially if we keep in mind that pre-equilibrium emission [2] of nucleons, as opposed to composite ejectiles, appears to be described relatively easily in a consistent way in terms of various formulations [3] which all share largely comparable insight of the relevant physical processes.

The effort of Koning *et al.* [4,5] to combine the best of current theoretical understanding of these reactions in a single computer program, represents one of the most ambitious projects to develop a robust and practicable means of quantitative calculations for a wide variety of pre-equilibrium reactions. Unfortunately, as implied earlier, with this theoretical application, more often than not, disconcerting disagreements between theoretical prediction and experimental data, for emission of heavier ejectiles such as ^3He , ^4He , etc., are encountered [6]. The origin of the problem is not obvious and various approaches to clarify the issue are possible. One option is to retain the basic ideas about the reaction mechanism as it has evolved from studies at lower incident energy, and then to refine details of calculations based on mechanisms which are known to become important [7] at higher incident energies. An alternative theoretical approach, such as in the work of Budzanowski *et al.* [8], is to invoke the extrapolation of a

totally different mechanism that results from studies at much higher incident energy, in the GeV range [9].

Most of the attempts to resolve the problem rely on studies of cross-section angular distributions, which are rather featureless. Consequently, the lack of any clear characteristic target mass or incident energy dependence evidently creates a difficulty. In principle, analyzing-power distributions are more sensitive to details of the reaction mechanism, and these were exploited in the past [10,11]. However, in practice measurements of analyzing-power data are rarer because they require beams of polarized particles. Nevertheless, it presents a greater challenge to the extraction of accurate quantities, especially at higher incident energies where cross section values drop considerably.

In several earlier investigations [10–13] of $(p, ^3\text{He})$ reactions at incident energies between 70 and 160 MeV it was assumed that the reaction mechanism is driven by a statistical intranuclear multistep process, with the ejectile emerging from two-nucleon pickup in the final stage. The theoretical analysis is based on the ideas of the multistep formulation of Feshbach, Kerman and Koonin [14], combined with a distorted wave Born approximation (DWBA) for the final pickup. Comparison between the theoretical predictions and experimental cross section and analyzing power angular distributions yields reasonable agreement.

In recent published work [11] we studied the $(p, ^3\text{He})$ reaction at incident energies between 100 and 160 MeV on ^{59}Co and ^{93}Nb . Note that in Ref. [11] it is mentioned that data were measured for ^{93}Nb also at an incident energy of 160 MeV, but no results were shown. The reason is that the analyzing power for ^{93}Nb at 160 MeV from that experiment suffered from such poor statistical accuracy, and covered such a small angular range, that it would have been meaningless to include them in Ref. [11]. The present work addresses the deficiency.

* Also at iThemba Laboratory for Accelerator Based Sciences, PO Box 722, Somerset West 7129, South Africa; aac@sun.ac.za

The two target nuclei ^{59}Co and ^{93}Nb were chosen in Ref. [11] as representative of medium to heavy mass nuclei in general, although detail differences, depending on the specific nucleus, are observed. It is encouraging that these differences seem to be predicted reasonably well by the theoretical treatment. Furthermore, the quenching of the analyzing power [15,16] as the incident energy is increased, is implicitly supported by the theory. However, due to the complicated and convoluted nature of the theory, the detailed reasons for the decreasing analyzing power towards higher incident energy are not understood yet.

In this paper we present new experimental and theoretical results for $^{93}\text{Nb}(p,^3\text{He})$ at an incident energy of 160 MeV in order to investigate consistency with our previous studies [10,11] and to gain additional insight. We previously presented a preliminary account of the results reported here at an international conference [17], but now we provide considerably more detail, as well as an account of the experimental and theoretical procedures that were followed.

In Sec. II the experimental setup and design considerations are presented. Section III comprises a brief overview of the salient features of the theoretical treatment, with a description of an improved method to generate appropriate distorted waves for the incident proton and the outgoing ^3He particle. The results are presented and discussed in Sec. IV. Finally, a summary and conclusions are given in Sec. V.

II. EXPERIMENTAL PROCEDURE

A beam of polarized protons \vec{p} (for simplicity we use the symbol p interchangeably also for polarized particles, as would be clear from the context) at an incident energy of 160 ± 0.5 MeV was delivered by the separated sector cyclotron of iThemba Laboratory for Accelerator Based Sciences (LABS), Faure, South Africa. The external polarized ion source feeds beam into an injector cyclotron that accelerates protons to a maximum energy of 8 MeV, with further acceleration in the main cyclotron. The accelerator system and the experimental equipment used in this study have been described elsewhere [18].

The experimental details and technique employed in the present investigation follow those described in our earlier work very closely [10,11], therefore only a brief description is given here. The experiment was performed inside a scattering chamber of 1.5 m diameter, with two detector telescopes each consisting of a $500\ \mu\text{m}$ silicon surface barrier detector followed by a NaI(Tl) crystal, connected to a photomultiplier tube. A standard ΔE - E particle identification technique was used to select ^3He ejectiles from the reaction in a target mounted at the center of the scattering chamber.

The two detector telescopes subtended the same nominal solid angles (1.13 msr) as defined by tantalum collimators thick enough to stop ^3He (approximately 3 mm thick with a 14 mm diameter hole). In order to cut down on the flux of lighter reaction products (protons, deuterons, and tritons) additional, slightly larger brass collimators were used in front of the telescopes. This setup was selected in order to minimize the

influence of undesirable collimator scattering of ^3He reaction products that could otherwise enter the detector telescopes.

Standard methods were followed to minimize systematic error on the measurement of the analyzing power. This entailed placing the two detector telescopes at symmetric scattering angles on opposite sides of the beam during data taking. In addition, the polarization of the incident protons (from 65% to 85% during the experiment), directed perpendicular to the scattering plane, was switched from up to down at 10 s intervals.

The polarization of the beam was determined regularly by scattering of the beam from a ^{12}C foil in the scattering chamber at 19° where the analyzing power for $p+^{12}\text{C}$ elastic scattering at 160 MeV is large (0.92) and accurately known [19]. The difference in the polarization between the two orientations was usually less than 10%, but different values as determined experimentally were used for the two polarization orientations to calculate analyzing power values.

Energy calibrations of the silicon surface barrier detectors were made using a ^{228}Th α -particle source, and the calibrations of the NaI(Tl) detector elements were based on the kinematics of the elastic scattering reactions $^1\text{H}(p, p)^1\text{H}$ and $^{12}\text{C}(p, p)^{12}\text{C}$ from a thin polyethylene target. These calibrations for protons in the telescope also provide energy values for ^3He , if the difference in the response of these ejectiles with the NaI(Tl) assembly is taken into account [20]. Gain drifts in the photomultiplier tubes of the NaI detectors were monitored by a light-emitting diode pulser system, which allowed corrections to be made during analysis. The overall uncertainty in the energy scale for ^3He is approximately 4%.

Two ^{93}Nb targets which were used, were both self-supporting foils of natural isotopic composition (100% occurrence of the isotope of interest) with thicknesses of 2.6 and 8.6 mg/cm^2 . The uncertainty in the thicknesses of the targets (up to 7%) is the main contribution to the systematic error on the cross section data.

Standard electronics were used and data were collected and monitored on an online system, and stored for subsequent offline replay of the data. Data were obtained for ^3He emission energies from a threshold of ≈ 30 MeV up to the kinematic limit and scattering angles from 15° to 60° (lab.) were covered.

III. THEORETICAL ANALYSIS

As in our previous work [10–12], we treat the $(p, ^3\text{He})$ reaction as occurring in a series of steps in which, as the simplest process leading to composite particle emission, the incident proton can pick up a nucleon pair directly from the target in a single step. Alternatively the pickup takes place after a variable number of intranuclear nucleon collisions. Consequently the multistep part may be two-step, three-step, etc. In our notation a two-step reaction is symbolically indicated as $(p, p', ^3\text{He})$ and a three-step reaction as $(p, p', p'', ^3\text{He})$.

The theory applied to the $(p, ^3\text{He})$ reaction is based on the multistep direct theory of Feshbach, Kerman, and Koonin (FKK) [14] for the intranuclear collisions leading up to the final two-nucleon pickup, which is then treated in the distorted wave Born approximation (DWBA). The extension of the FKK

theory from cross sections to analyzing power is given by Bonetti *et al.* [21].

The theoretical formulation has been described extensively in our earlier publications and references therein. Nevertheless, in order to highlight some improvements and subtle modifications introduced in this work, and for ease of use to the reader, we reproduce a comprehensive account of the theory in the description that follows. For clarity we use the same notation as in Ref. [11].

A. Differential cross sections

The double-differential cross section is written as a function of solid angle $d\Omega$ and emission energy dE acceptance. This is expressed as

$$\frac{d^2\sigma}{d\Omega dE} = \left(\frac{d^2\sigma}{d\Omega dE}\right)^{1\text{-step}} + \left(\frac{d^2\sigma}{d\Omega dE}\right)^{2\text{-step}} + \dots, \quad (1)$$

where, as mentioned earlier, the first step cross section is taken as a direct two-nucleon ($p, {}^3\text{He}$) pickup process calculated in terms of the DWBA. This term is given by

$$\left(\frac{d^2\sigma}{d\Omega dE}\right)^{1\text{-step}} = \sum_{N,L,J} \frac{(2J+1)}{\Delta E} \frac{d\sigma^{\text{DW}}}{d\Omega}(\theta, N, L, J, E), \quad (2)$$

at scattering angle θ , where the summation runs over the target states with single-particle energies within a small interval ($E - \Delta E/2, E + \Delta E/2$) around the excitation energy E . The two-nucleon system bound in the target has quantum numbers N, L , and J , as will be specified later.

The last factor in Eq. (2) is the DWBA differential cross section, which is expressed as [22,23]

$$\begin{aligned} & \frac{d\sigma^{\text{DW}}}{d\Omega}(\theta, N, L, J, E) \\ &= \mathcal{N} \sum_{\{n_k\}} G^2(\{n_k\})^2 \frac{2J_f + 1}{2J_i + 1} \sum_{T=0,1} b_{\text{ST}}^2 D_{\text{ST}}^2 \\ & \times \langle T_f T_{fz} T T_z | T_i T_{iz} \rangle^2 \left(\frac{d\sigma}{d\Omega}\right)^{\text{DWUCK}}, \end{aligned} \quad (3)$$

where the sum runs over all possible neutron-proton configurations $\{n_k\}$. Here \mathcal{N} is a normalization constant whose value depends on the square of the fractional parentage coefficient for the two-nucleon removal [24] as well as the optical model potentials. The quantity $G^2(\{n_k\})^2$ is the spectroscopic factor for a proton and neutron to form a deuteron bound state with quantum numbers (N, L, J) , and S and T are the transferred spin and isospin, respectively, with the selection rule $S + T = 1$. Because the microscopic calculation of the pickup of a neutron-proton pair gives essentially the same result as a macroscopic calculation in which the nucleon pair is treated as a deuteron cluster [23], we consider the target nucleus to consist of a core to which a deuteron is bound in a shell-model state. The reaction can then be described as a direct transition of a deuteron, considered as a single particle. The final and initial total angular momenta are indicated by J_f and J_i , respectively.

The quantity b_{ST}^2 is 0.5 for both values of S and T , and the values for the strengths of the proton-deuteron interaction D_{10}^2 and D_{01}^2 are 0.3 and 0.72, respectively [25]. The square of the Clebsch–Gordan coefficient depends on initial, transferred and final isospins T_i, T , and T_f . The differential cross sections $(\frac{d\sigma}{d\Omega})^{\text{DWUCK}}$ to particular (N, L, J, T) states are calculated using the code DWUCK4 [26].

The form factor of the deuteron is obtained by the usual procedure of adjusting the well depth of a Woods-Saxon potential with geometrical parameters $r_0 = 1.15$ fm and $a = 0.76$ fm [27,28] to obtain the correct binding energy and wave function characteristics. As was implied earlier, this geometry results in macroscopic form factors that resemble the microscopic ones very closely, as would be required.

The multistep cross sections, which are appropriate for the second and higher steps of the ($p, {}^3\text{He}$) reaction, are expressed as

$$\begin{aligned} & \left(\frac{d^2\sigma}{d\Omega dE}\right)^{\text{multistep}} \\ &= \sum_{n=2}^{n_{\text{max}}} \sum_{m=n-1}^{n+1} \int \frac{d\mathbf{k}_1}{(2\pi)^3} \int \frac{d\mathbf{k}_2}{(2\pi)^3} \dots \int \frac{d\mathbf{k}_n}{(2\pi)^3} \\ & \times \left(\frac{d^2\sigma(\mathbf{k}_f, \mathbf{k}_n)}{d\Omega_f dE_f}\right) \times \left(\frac{d^2\sigma(\mathbf{k}_n, \mathbf{k}_{n-1})}{d\Omega_n dE_n}\right) \times \dots \\ & \times \left(\frac{d^2\sigma(\mathbf{k}_2, \mathbf{k}_1)}{d\Omega_2 dE_2}\right) \times \left(\frac{d^2\sigma(\mathbf{k}_1, \mathbf{k}_i)}{d\Omega_1 dE_1}\right)^{1\text{-step}}_{p,p'}, \end{aligned} \quad (4)$$

where $\mathbf{k}_i, \mathbf{k}_n$, and \mathbf{k}_f are the momenta of the initial, n th, and final steps. The number of reaction steps is indicated with the symbol n , the maximum number of reaction steps is n_{max} and m is the exit mode. Therefore the cross section associated with m is given by the two-nucleon pickup reaction leading to the emission of ${}^3\text{He}$, and all steps prior to the final step are nucleon-nucleon collisions.

As was pointed out before [11], the specific structure of the formalism facilitates separate calculation of multistep processes, such as two-step ($p, p', {}^3\text{He}$) and three-step ($p, p', p'', {}^3\text{He}$) reactions. Of course, as in previous work [10,11], we do not allow the possibility of a ($p, n, {}^3\text{He}$) contribution, which corresponds to the pickup of a diproton. Nevertheless, inclusion of different nucleons on an equal footing in the multistep part of the reaction could be approximately compensated for by a renormalization of the relevant (p, p') and (p, p', p'') cross sections. However, such an adjustment would affect only the global overall normalization factor, which becomes irrelevant when the magnitude of the theoretical cross section is refitted to the experimental data anyway, as will be explained later.

The theoretical (p, p') and (p, p', p'') double-differential cross-section distributions which are required to calculate the contributions of the second- and third-step processes were derived from Refs. [29,30]. These cross-section distributions were extracted by means of a FKK multistep direct reaction theory, which reproduce experimental inclusive (p, p') quantities [30] on target nuclei which are close to those needed for this work, and in an appropriate incident energy range. Interpolations and extrapolations in incident energy and target

mass were introduced to match the specific requirements accurately.

It should be noted that the theory contains an overall normalization constant \mathcal{N} , as expressed in Eq. (3), which we adjust to reproduce the experimental cross-section angular distribution at a high emission energy where the one-step reaction dominates. This procedure is best from a theoretical point of view, because the accumulated uncertainty resulting from our specific choice of input ingredients in the formulation would be less than for the higher order steps. Of course, as we will see, the analyzing power is a ratio of cross sections, therefore it does not depend on the value of this normalization constant.

B. Analyzing power distributions

The analyzing power in terms of protons polarized to a value P_+ in the positive (up) direction as defined by the Basel [31] and Madison [32] conventions, is given by

$$A_y = \frac{1}{P_+} \left(\frac{\sigma_L - \sigma_R}{\sigma_L + \sigma_R} \right), \quad (5)$$

where σ_L and σ_R are the double-differential cross sections for the emission of hellions to the left L and right R of the incident particle beam, respectively. An analogous expression holds when the proton polarization is flipped relative to the scattering plane. A fully polarized beam has a magnitude of unity.

The multistep expression for the analyzing power becomes

$$A_{\text{multistep}} = \frac{A_1 \left(\frac{d^2\sigma}{d\Omega dE} \right)^{1\text{-step}} + A_2 \left(\frac{d^2\sigma}{d\Omega dE} \right)^{2\text{-step}} + \dots}{\left(\frac{d^2\sigma}{d\Omega dE} \right)^{1\text{-step}} + \left(\frac{d^2\sigma}{d\Omega dE} \right)^{2\text{-step}} + \dots}, \quad (6)$$

with A_i , $\{i = 1, 2, \dots\}$ referring to analyzing powers for the successive multisteps.

C. Optical potentials in the DWBA calculation

Important ingredients in the theoretical description of the nuclear reaction properties are the optical potentials, which take into account the interaction between projectile and target, and between the ejectile and the heavy residual nucleus, respectively. The potentials contain volume V and spin-orbit V_{SO} parts, which are both complex in general, expressed as

$$U(\mathbf{r}) = V(\mathbf{r}) + V_{\text{SO}}(\mathbf{r}) \mathbf{L} \cdot \mathbf{S}, \quad (7)$$

where r is the relative radial coordinate, \mathbf{L} the angular momentum, and \mathbf{S} the intrinsic spin of the projectile.

In our previous studies [10,11] we have used the global optical potential of Madland and Schwandt [33,34] for protons and a double folding potential based on the DDMY3 effective interaction [35,36] for ^3He .

In this work we treat the volume part of the optical potentials in the incident and the outgoing channels on the same footing by application of the hybrid nucleus-nucleus optical potential.

The hybrid nucleus-nucleus optical potential [37] has real and imaginary parts:

$$U(\mathbf{r}) = N^R V^{\text{DF}}(\mathbf{r}) + i N^I W(\mathbf{r}) \quad (8)$$

which generally depend on the radius-vector \mathbf{r} connecting centers of the interacting nuclei. The parameters N^R and N^I correct the strength of the microscopically calculated real V^{DF} and imaginary W constituents of the whole potential.

The real part V^{DF} is that double-folding potential that consists of direct and exchange components:

$$V^{\text{DF}}(\mathbf{r}) = V^D(\mathbf{r}) + V^{\text{EX}}(\mathbf{r}) \quad (9)$$

with

$$V^D(\mathbf{r}) = \int d\mathbf{r}_p d\mathbf{r}_t \rho_p(\mathbf{r}_p) \rho_t(\mathbf{r}_t) v_{NN}^D(\mathbf{s}), \quad (10)$$

$$V^{\text{EX}}(\mathbf{r}) = \int d\mathbf{r}_p d\mathbf{r}_t \rho_p(\mathbf{r}_p, \mathbf{r}_p + \mathbf{s}) \rho_t(\mathbf{r}_t, \mathbf{r}_t - \mathbf{s}) \times v_{NN}^{\text{EX}}(\mathbf{s}) \exp \left[\frac{i \mathbf{K}(\mathbf{r}) \cdot \mathbf{s}}{M} \right], \quad (11)$$

where $\mathbf{s} = \mathbf{r} + \mathbf{r}_t - \mathbf{r}_p$ is the vector between the projectile and target nucleons. The reduced mass coefficient is $M = A_p A_t / (A_p + A_t)$, where A_p and A_t refer to the projectile and target atomic mass numbers. The quantities $\rho_p(\mathbf{r}_p)$ and $\rho_t(\mathbf{r}_t)$ are their density distributions, $\rho_p(\mathbf{r}_p, \mathbf{r}_p + \mathbf{s})$ and $\rho_t(\mathbf{r}_t, \mathbf{r}_t - \mathbf{s})$ are the density matrices, which are approximated as in Ref. [38]. The effective NN potentials v_{NN}^D (of CDM3Y6-type) are based on the Paris NN potential:

$$v_{NN}^D(E, \rho, s) = g(E) F(\rho) \sum_{i=1}^3 N_i \frac{\exp(-\mu_i s)}{\mu_i s}. \quad (12)$$

The energy and density dependencies are, respectively,

$$g(E) = 1 - 0.003E/A_p, \quad F(\rho) = C[1 + \alpha e^{-\beta\rho} - \gamma\rho], \quad (13)$$

$$\rho = \rho_p(\mathbf{r}_p) + \rho_t(\mathbf{r}_t).$$

The parameters in Eqs. (12) and (13) are defined in Ref. [39]. For the incident channel calculations, ρ_t for ^{93}Nb was taken as the standard Fermi form, with parameters from [40]. For the exit channel, a modified harmonic oscillator expression $\rho_p = 0.108 \exp(-0.3425r^2)$ was used for ^3He , whereas a three-parameter Gaussian with parameters from Ref. [40] was used for ^{91}Zr .

One should note that in Eq. (11) the radial part of the nucleus-nucleus momentum $K(r)$ depends on the folding potential $V^{\text{DF}}(r)$ itself:

$$K(r) = \left\{ \frac{2Mm}{\hbar^2} [E - V^{\text{DF}}(r) - V_c(r)] \right\}^{1/2}, \quad (14)$$

where V_c is the Coulomb potential, M as defined earlier, and m is the nucleon mass. Evidently the calculation of the folding potential V^{DF} in Eq. (9) is a typical nonlinear problem.

The imaginary part of the optical potential $W(\mathbf{r})$ in Eq. (8) may have the same form as its real counterpart V^{DF} , or can be calculated separately within the high-energy approximation [41] as it was developed in Ref. [37].

The microscopic optical potential obtained in the high-energy approximation in the momentum space has the

form

$$U_{\text{opt}}^H(\mathbf{r}) = -\frac{E}{k} \bar{\sigma}_N (i + \bar{\alpha}_N) \frac{1}{(2\pi)^3} \times \int d\mathbf{q} e^{-i\mathbf{q}\cdot\mathbf{r}} \rho_p(\mathbf{q}) \rho_t(\mathbf{q}) f_N(q). \quad (15)$$

Here the NN total scattering cross section $\bar{\sigma}_N$ and the ratio of real to imaginary parts of the forward NN amplitude $\bar{\alpha}_N$ are averaged over the isospins of the nuclei. They are parameterized as given in Refs. [42,43]. The NN form factor is taken as $f_N(q) = \exp(-q^2\beta/2)$ with the slope parameter $\beta = 0.219 \text{ fm}^2$ [44]. In fact, we used only the imaginary part of Eq. (15) transformed to the form

$$W^H(r) = -\frac{1}{2\pi^2} \frac{E}{k} \bar{\sigma}_N \int_0^\infty j_0(qr) \rho_p(q) \rho_t(q) f_N(q) q^2 dq. \quad (16)$$

Details about the calculations of the hybrid optical potential are presented in Refs. [37,39,45,46].

The hybrid optical potential as described above has been already successfully applied, e.g., in Refs. [47–49] for the analysis of elastic scattering data of light exotic nuclei.

It turned out that the shape of the analyzing power is rather sensitive to the spin-orbit part of the optical potential both in the incident and the outgoing channels. Consequently care had to be taken in the selection of appropriate potentials. Good agreement with the experimental data was obtained by using for protons (incident channel) a Woods-Saxon shape of the real and imaginary part of $V_{\text{SO}}(r)$. The parameters are those, listed in Ref. [50]. For the spin-orbit potential of ^3He (outgoing channel), on the other hand, we used the real volume part of the folding potential Eq. (9). The renormalization constants N^R and N^I in Eq. (8) in the incident channel are kept equal to unity, while their values for the exit channel were adjusted to follow the emission-energy trend of the experimental analyzing power data (see Table I).

Our treatment of N^R and N^I in the outgoing channel as free parameters which are fitted to the data, is consistent with the procedure followed in Ref. [49]. The values found in our present investigation, and the trend observed as a function of emission energy, need further theoretical analysis and complementary experimental studies for proper evaluation and interpretation.

The last coefficient we have used to reproduce the experimental data for the double-differential cross section for the one-step reaction is \mathcal{N} in Eq. (3). The value that we needed to fit the data at $E_{\text{out}} = 150 \text{ MeV}$, where the direct transfer reaction is the most probable, is $\mathcal{N} = 0.12$. It is kept constant for all calculations of the one-step reaction cross sections.

TABLE I. Values of the renormalization constants N^R and N^I in Eq. (8) for the outgoing channel.

E_{out} (MeV)	150	126	102	82
N^R	0.5	0.3	0.25	0.25
N^I	0.0	0.01	0.05	0.08

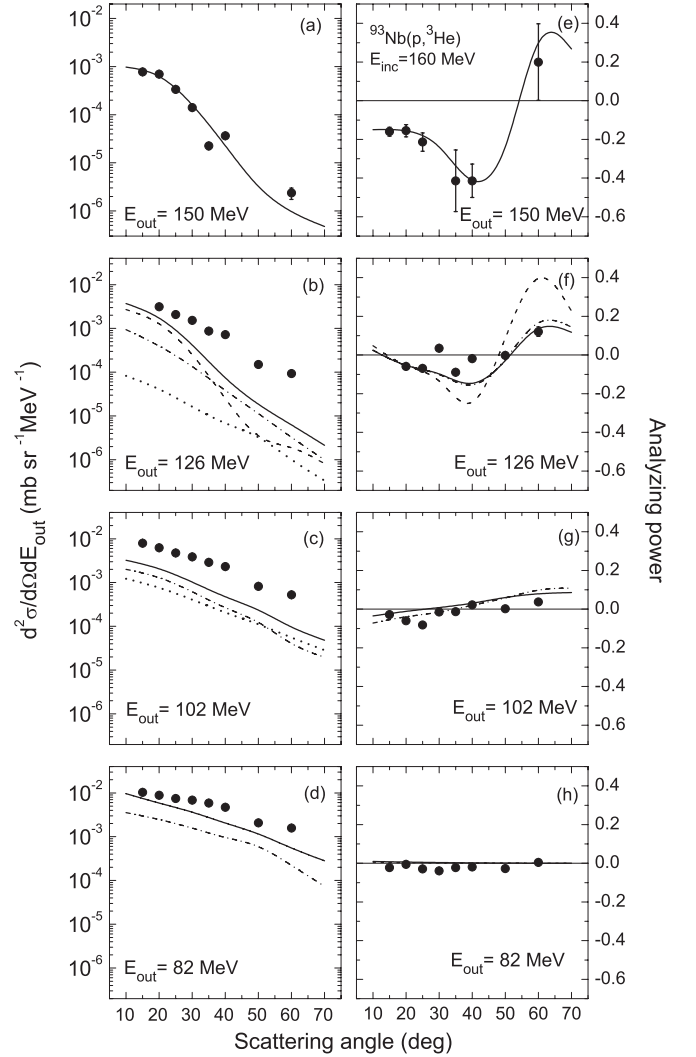


FIG. 1. Double-differential cross sections (a)–(d) and analyzing power (e)–(h) as a function of scattering angle θ for the $^{93}\text{Nb}(p, ^3\text{He})$ reaction at an incident energy of 160 MeV and various ^3He outgoing energies E_{out} as indicated. Theoretical cross section calculations for one step (---) two steps (- · - · -), and three steps (· · · · ·) are shown, with the sums of the contributions plotted as continuous curves. The experimental analyzing power distributions are compared with theoretical calculations for a one-step reaction (---), a one-step plus a two-step reaction (- · - · -), and a one- plus two- plus three-step reaction (solid lines).

IV. RESULTS

Double-differential cross-section and analyzing-power angular distributions for the $^{93}\text{Nb}(p, ^3\text{He})$ reaction at an incident energy of 160 MeV are displayed in Fig. 1 for various outgoing energies of ^3He . The theory reproduces the experimental quantities reasonably well, especially if we keep in mind that the accuracy of the calculations is limited to some extent by uncertainties inherent to the input ingredients of the theory, as implied in Sec. III.

All the theoretical cross section distributions were normalized with a single factor extracted from the angular distribution at an emission energy E_{out} of 150 MeV, for which the one-step

reaction dominates. As explained in Sec. III, this procedure is based on theoretical considerations. However, experimental uncertainties in, for example, the emission energy calibration would result in a systematic error in the cross section which is worst at the top end of emission energies. Consequently, the fact that the cross sections appear to be mostly underestimated by the theory could merely be an artifact of our normalization procedure. Within these constraints, the overall agreement for the cross section angular distributions is nevertheless satisfactory. Of course, as was mentioned earlier, the analyzing power is unaffected by this.

The value used to display the theoretical double-differential cross section data in Fig. 1 is $\mathcal{N} = 0.12$. One may speculate that this value is relevant to the preformation factor of the deuteron in the target nucleus, but proof of such a relationship would require extensive additional systematic studies. Nevertheless, in any such interpretation one should keep in mind that our model of the picked up nucleon pair as a deuteron is merely a matter of convenience, which gives approximately the same result as a microscopic treatment.

As in our previous work [10–12], and as expected for the multistep character of the reaction process, the dominant step in the chain changes drastically as a function of emission energy. This has a profound influence on the features of the analyzing power angular distributions, and to a lesser extent to those of the cross section distributions.

At the incident energy of 160 MeV of the present work, the analyzing power of the $^{93}\text{Nb}(p,^3\text{He})$ reaction approaches zero very rapidly as the emission energy drops. It should be noted that results are only shown down to an emission energy of 82 MeV in Fig. 1, but below this outgoing energy the analyzing power remains essentially zero, as was explicitly shown in our preliminary report of this work [17].

To a large extent a decreasing analyzing power towards lower emission energy and larger scattering angles is a natural phenomenon associated with the multistep character of the reaction mechanism, and in itself is therefore not surprising. However, why such a trend should become especially drastic as the incident energy is increased, is not obvious.

The drop in analyzing power as the incident energy is increased from, say 100 MeV to 200 MeV, appears to be well established [11,15,16], and although only a few nuclear species have been investigated to date, it seems to hold generally. An illustration of this quenching of the analyzing power with increasing incident energy is provided in Fig. 2, where an energy distribution from this work for the $^{93}\text{Nb}(p,^3\text{He})$ reaction at a scattering angle of 40° is compared with one from Ref. [10] at the same scattering angle, but at a lower incident energy of 100 MeV. Within the limitation of the theoretical implementation, the calculations track the experimental analyzing power distributions in Fig. 2 as accurately as would be expected. Thus the observed trend is reproduced by the theory, in spite of the fact that a simple reason for the quenching remains obscure.

From this work, together with our previous studies [10,11], it is known that there is a clear correlation between low values of analyzing power and the relative importance of multistep contributions in the explored incident energy range.

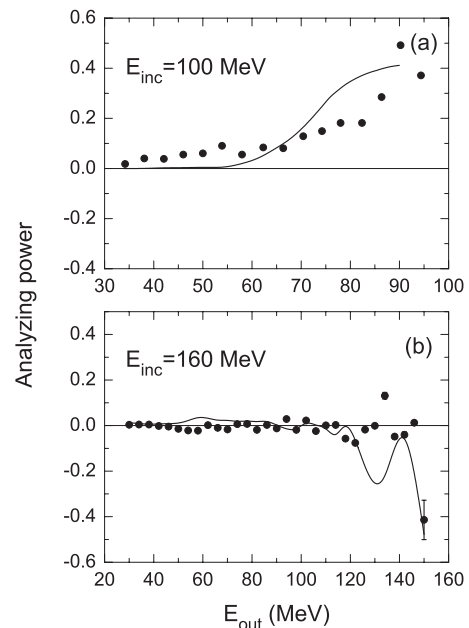


FIG. 2. Emission energy distributions of the analyzing power for the reaction $^{93}\text{Nb}(p,^3\text{He})$ at a scattering angle θ of 40 degrees at incident energies of 100 (a) and 160 MeV (b). The curves represent theoretical calculations which include a total of up to three steps. Note that the energy scales are different on the upper and lower panels. The experimental and theoretical results at an incident energy of 100 MeV are derived from Ref. [10].

Consequently, it is reasonable to expect that the observed quenching of the analyzing power towards higher incident energy is also related to the influence of higher steps in the reaction process. However, Cowley [51] showed that the first-step contribution drops off considerably more slowly with increasing incident energy than the higher steps. In other words, higher steps should influence the analyzing power less, instead of more, as the incident energy is increased. This suggests that the incident-energy dependence of the quenching may perhaps be linked to the trend of the first step itself. Unfortunately, due to the convoluted nature of the theoretical expression for the analyzing power, it is difficult to quantify the origin of the observed phenomenon from the results of the present experiment. Therefore, in order to investigate the behavior of the single-step analyzing power further, a new study [52] is planned in which the $(p,^3\text{He})$ direct reaction to discrete final states with known spins and parities will be measured.

In the present work we have extended our earlier investigation [11] to a complete study for $^{93}\text{Nb}(p,^3\text{He})$ at an incident energy of 160 MeV, which can now be compared with results at lower incident energy. This allows the implicit assumption in our earlier work, that ^{93}Nb should behave analogously to ^{59}Co at the highest energy, to be confirmed. The new results are found to be consistent with those from lower incident energies [10,11]. Furthermore, although detailed differences are encountered for this target nucleus compared to ^{59}Co [11], as would be expected, the basic reaction mechanism clearly remains similar.

V. SUMMARY AND CONCLUSIONS

The reaction $^{93}\text{Nb}(p,^3\text{He})$ at an incident energy of 160 MeV leading to ejectiles into the continuum of excitation, was investigated. Double-differential cross section and analyzing power angular distributions were measured between 15° and 60° at various emission energies.

The experimental results were investigated in terms of a statistical multistep formulation in which each individual sequence of steps may end up with emission of ^3He . The ejectile is assumed to originate from a two-nucleon pickup process in the terminal stage. The theoretical predictions are in reasonable agreement with the angular distributions of the measured quantities. This study gives a description of the $(p,^3\text{He})$ reaction on ^{93}Nb which is consistent with the published interpretation at lower incident energies down to 100 MeV.

Together with the earlier work, information regarding the $(p,^3\text{He})$ reaction on ^{93}Nb now extends to the same incident energy range between 100 and 160 MeV as for the target nucleus ^{59}Co . Therefore, it is possible to compare existing insight into the reaction mechanism from the $^{59}\text{Co}(p,^3\text{He})$ reaction with conclusions derived from the complete set of analyses for ^{93}Nb . Analogous features are found to characterize the $(p,^3\text{He})$ reaction on these two target nuclei.

The well-established quenching of the analyzing power with increasing incident energy is confirmed and clearly manifested in the present investigation. It appears likely that this result is a natural outcome of the incident-energy dependence of a direct reaction that is driven by a multistep mechanism. Unfortunately the use of analyzing power to unravel the reaction mechanism of nucleon-induced pre-equilibrium composite particle emission appears to diminish beyond the incident energy investigated in this study.

Clearly it is desirable to conduct further experiments on a wider range of target nuclei. Also, further theoretical refinement and development would be invaluable.

ACKNOWLEDGMENTS

We thank Professor V. K. Lukyanov for his valuable guidance during the development of the formulation of the folding potentials. The research of A.A.C. was funded by the National Research Foundation (NRF) of South Africa. The studies of S.S.D. were partially supported by grant no. D-02-285 of the Bulgarian Science Foundation. E.V.Z. and K.V.L. were supported by the Russian Foundation for Basic Research (RFBR) under Grant No. 12-01-00396a. This financial support is gratefully acknowledged.

-
- [1] D. S. Ginger, K. Kwiatkowski, G. Wang, W.-c. Hsi, S. Hudan, E. Cornell, R. T. de Souza, V. E. Viola, and R. G. Korteling, *Phys. Rev. C* **78**, 034601 (2008).
- [2] E. Gadioli and P. E. Hodgson, *Pre-Equilibrium Nuclear Reactions* (Oxford University Press, New York, 1991).
- [3] A. J. Koning and J. M. Akkermans, *Phys. Rev. C* **47**, 724 (1993).
- [4] A. J. Koning and M. C. Duijvestijn, *Nucl. Phys. A* **744**, 15 (2004).
- [5] A. J. Koning, S. Hilaire, and M. C. Duijvestijn, TALYS-1.0, in *Proceedings of the International Conference on Nuclear Data for Science and Technology, Nice, France, 2007*, edited by O. Bersillon, F. Gunsing, E. Bauge, R. Jacqmin, and S. Leray (EDP Sciences, Les Ulis, France, 2008), pp. 211–214.
- [6] R. Bevilacqua, Ph.D. thesis, Uppsala University, 2011.
- [7] C. Kalbach, *Phys. Rev. C* **71**, 034606 (2005).
- [8] A. Budzanowski, M. Fidelus, D. Filges, F. Goldenbaum, H. Hodde, L. Jarczyk, B. Kamys, M. Kistryn, St. Kistryn, St. Kliczewski, A. Kowalczyk, E. Kozik, P. Kulesa, H. Machner, A. Magiera, B. Piskor-Ignatowicz, K. Pysz, Z. Rudy, R. Siudak, and M. Wojciechowski, *Phys. Rev. C* **80**, 054604 (2009).
- [9] A. Budzanowski, M. Fidelus, D. Filges, F. Goldenbaum, H. Hodde, L. Jarczyk, B. Kamys, M. Kistryn, St. Kistryn, St. Kliczewski, A. Kowalczyk, E. Kozik, P. Kulesa, H. Machner, A. Magiera, B. Piskor-Ignatowicz, K. Pysz, Z. Rudy, R. Siudak, and M. Wojciechowski, *Phys. Rev. C* **82**, 034605 (2010).
- [10] A. A. Cowley, G. F. Steyn, S. S. Dimitrova, P. E. Hodgson, G. J. Arendse, S. V. Försch, G. C. Hillhouse, J. J. Lawrie, R. Neveling, W. A. Richter, J. A. Stander, and S. M. Wyngaardt, *Phys. Rev. C* **62**, 064605 (2000).
- [11] A. A. Cowley, J. Beuzidenhout, S. S. Dimitrova, P. E. Hodgson, S. V. Försch, G. C. Hillhouse, N. M. Jacobs, R. Neveling, F. D. Smit, J. A. Stander, G. F. Steyn, and J. J. van Zyl, *Phys. Rev. C* **75**, 054617 (2007).
- [12] A. A. Cowley, G. J. Arendse, G. F. Steyn, J. A. Stander, W. A. Richter, S. S. Dimitrova, P. Demetriou, and P. E. Hodgson, *Phys. Rev. C* **55**, 1843 (1997).
- [13] K. Spasova, S. S. Dimitrova, and P. E. Hodgson, *J. Phys. G* **26**, 1489 (2000).
- [14] H. Feshbach, A. Kerman, and S. Koonin, *Ann. Phys. (NY)* **125**, 429 (1980).
- [15] A. A. Cowley, J. Beuzidenhout, E. Z. Buthelezi, S. S. Dimitrova, S. V. Försch, G. C. Hillhouse, P. E. Hodgson, N. M. Jacobs, R. Neveling, F. D. Smit, J. A. Stander, G. F. Steyn, and J. J. van Zyl, in *Proceedings of the 23rd International Nuclear Physics Conference, INPC2007, Tokyo, Japan, 2007*, edited by S. Nagamiya, T. Motobayashi, M. Oka, R. S. Hayano, and T. Nagae Vol. 2 (Elsevier, Amsterdam, 2008), p. 473.
- [16] E. Renshaw, S. J. Yennello, K. Kwiatkowski, R. Planeta, L. W. Woo, and V. E. Viola, *Phys. Rev. C* **44**, 2618 (1991).
- [17] A. A. Cowley, S. S. Dimitrova, and J. J. van Zyl, in *Proceedings of the 3rd International Conference on Frontiers in Nuclear Structure, Astrophysics, and Reactions, Rhodes, Greece, 2010*, edited by P. Demetriou, R. Julin, and S. Harissopoulos [AIP Conf. Proc. No. 1377 (AIP, New York, 2010)], p. 69.
- [18] J. V. Pilcher, A. A. Cowley, D. M. Whittall, and J. J. Lawrie, *Phys. Rev. C* **40**, 1937 (1989).
- [19] H. O. Meyer, P. Schwandt, W. W. Jacobs, and J. R. Hall, *Phys. Rev. C* **27**, 459 (1983).
- [20] D. M. Whittall, A. A. Cowley, J. V. Pilcher, S. V. Försch, F. D. Smit, and J. J. Lawrie, *Phys. Rev. C* **42**, 309 (1990).
- [21] R. Bonetti, L. Colli Milazzo, I. Doda, and P. E. Hodgson, *Phys. Rev. C* **26**, 2417 (1982).
- [22] J. N. Bishop, L. R. Medsker, H. T. Fortune, and B. H. Wildenthal, *Phys. Rev. C* **20**, 1221 (1979).
- [23] J. S. Sens and R. J. de Meijer, *Nucl. Phys. A* **407**, 45 (1983).
- [24] E. Gadioli and E. Gadioli Erba, *J. Phys. G* **8**, 83 (1982).

- [25] H. Nann, W. Benenson, W. A. Lanford, and B. H. Wildenthal, *Phys. Rev. C* **10**, 1001 (1974).
- [26] P. D. Kunz and E. Rost in *Computational Nuclear Physics*, edited by K. Langanke *et al.*, Vol. 2 (Springer-Verlag, Berlin, 1993), Chap. 5.
- [27] R. J. de Meijer, L. W. Put, and J. C. Vermeulen, *Phys. Lett. B* **107**, 14 (1981).
- [28] R. J. de Meijer, L. W. Put, J. J. Akkermans, J. C. Vermeulen, and C. R. Bingham, *Nucl. Phys. A* **386**, 200 (1982).
- [29] A. A. Cowley, G. J. Arendse, J. W. Koen, W. A. Richter, J. A. Stander, G. F. Steyn, P. Demetriou, P. E. Hodgson, and Y. Watanabe, *Phys. Rev. C* **54**, 778 (1996).
- [30] W. A. Richter, A. A. Cowley, G. C. Hillhouse, J. A. Stander, J. W. Koen, S. W. Steyn, R. Lindsay, R. E. Julies, J. J. Lawrie, J. V. Pilcher, and P. E. Hodgson, *Phys. Rev. C* **49**, 1001 (1994).
- [31] P. Huber and K. P. Meyer, *Proceedings of the First International Symposium on Polarization Phenomena of Nucleons, Basel, Switzerland, 1960* (Springer-Verlag, New York, 1961).
- [32] H. H. Barschall and W. Haerberli, *Proceedings of the Third International Symposium on Polarization Phenomena in Nuclear Reactions, Madison, Wisconsin, USA, 1970* (University of Wisconsin Press, Madison, 1971).
- [33] D. G. Madland, in *Proceedings of Specialists' Meeting on Pre-Equilibrium Reactions, Semmering, Austria, 1988*, edited by B. Strohmaier (OECD, Paris, 1988), p. 103; International Atomic Energy Report No. IAEA-TECDOC-483, 1980, p. 80 (unpublished).
- [34] P. Schwandt, H. O. Meyer, W. W. Jacobs, A. D. Bacher, S. E. Vigdor, M. D. Kaitchuck, and T. R. Donoghue, *Phys. Rev. C* **26**, 55 (1982).
- [35] A. M. Kobos, B. A. Brown, P. E. Hodgson, G. R. Satchler, and A. Budzanowski, *Nucl. Phys. A* **384**, 65 (1982).
- [36] Y. Sakuragi and M. Katsuma, *Nucl. Instrum. Methods Phys. Res. A* **402**, 347 (1998).
- [37] V. K. Lukyanov, E. V. Zemlyanaya, and K. V. Lukyanov, JINR Preprint P4-2004-115, Dubna, 2004; *Phys. At. Nucl.* **69**, 240 (2006).
- [38] J. W. Negele and D. Vautherin, *Phys. Rev. C* **5**, 1472 (1972).
- [39] D. T. Khoa and G. R. Satchler, *Nucl. Phys. A* **668**, 3 (2000).
- [40] J. D. Patterson and R. J. Peterson, *Nucl. Phys. A* **717**, 235 (2003).
- [41] R. J. Glauber, *Lectures in Theoretical Physics* (Interscience, New York, 1959), p. 315.
- [42] S. K. Charagi and S. K. Gupta, *Phys. Rev. C* **41**, 1610 (1990); **46**, 1982 (1992).
- [43] P. Shukla, [arXiv:nucl-th/0112039](https://arxiv.org/abs/nucl-th/0112039).
- [44] G. D. Alkhazov, S. L. Belostotsky, and A. A. Vorobyov, *Phys. Rep.* **42**, 89 (1978).
- [45] K. V. Lukyanov, Comm. JINR, P11-2007-38, Dubna, 2007.
- [46] P. Shukla, *Phys. Rev. C* **67**, 054607 (2003).
- [47] K. V. Lukyanov, V. K. Lukyanov, E. V. Zemlyanaya, A. N. Antonov, and M. K. Gaidarov, *Eur. Phys. J. A* **33**, 389 (2007).
- [48] V. K. Lukyanov, E. V. Zemlyanaya, K. V. Lukyanov, D. N. Kadrev, A. N. Antonov, M. K. Gaidarov, and S. E. Massen, *Phys. Rev. C* **80**, 024609 (2009).
- [49] V. K. Lukyanov, D. N. Kadrev, E. V. Zemlyanaya, A. N. Antonov, K. V. Lukyanov, and M. K. Gaidarov, *Phys. Rev. C* **82**, 024604 (2010).
- [50] R. L. Walter and P. P. Guss, in *Proceedings of the International Conference on Nuclear Data for Basic and Applied Science, Santa Fe, 1985*, edited by P. G. Young (Gordon and Breach, New York, 1986), p. 1079.
- [51] A. A. Cowley, in *Proceedings of the 28th International Workshop on Nuclear Theory, Rila Mountains, Bulgaria, June 2009*, Nuclear Theory Vol. 28, edited by S. S. Dimitrova (INRNE, Sofia, Bulgaria, 2009), p. 35.
- [52] J. J. van Zyl, Ph.D. thesis, Stellenbosch University, 2012 (unpublished).